UNPUBLISHED PRELIMINARY DATA

SEMIANNUAL STATUS REPORT NO. 4
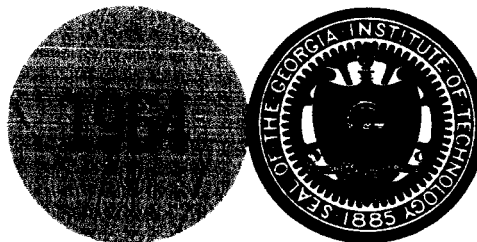
PROJECT NO. A-635

N64-26361

Code-1

nasa CR-58058

Cat. 13

HEAT TRANSFER TO A GAS
CONTAINING A CLOUD OF PARTICLES

Andrew McAlister, Henderson C. Ward, Alberto F. Hidalgo,
and Clyde Orr, Jr.

Covering the Period
1 December 1963 to 31 May 1964
Printed 25 June 1964

OTS PRICE

XEROX $ 4.60 ph.

MICROFILM $ _____

REPORTS CONTROL No. 1

GEORGIA INSTITUTE OF TECHNOLOGY
Engineering Experiment Station
Atlanta, Georgia

SEMIANNUAL STATUS REPORT NO. 4

PROJECT NO. A-635

HEAT TRANSFER TO A GAS
CONTAINING A CLOUD OF PARTICLES

By

ANDREW MCALISTER, HENDERSON C. WARD,
ALBERTO F. HIDALGO, and CLYDE ORR, JR.

Covering the Period
1 December 1963 to 31 May 1964
Printed 2 July 1964

Prepared for
NATIONAL AERONAUTICS AND SPACE ADMINISTRATION
WASHINGTON, D.C. 20005

TABLE OF CONTENTS

This report contains 42 pages.

LIST OF FIGURES

LIST OF TABLES

I. SUMMARY

The objective of this investigation is to study the thermal behavior of particle clouds during exposure to radiant energy and, by means of experimental measurements and theoretical analyses, to investigate methods for describing quantitatively the basic process involved. It is anticipated that the results will be useful in applied problems.

⌊The radiant energy absorbed by particle clouds was measured while the clouds were flowing inside a quartz tube through the walls of which energy was being received from surrounding radiators.⌋ The apparatus has previously been described in detail. Experiments were performed during the first part of this report period to characterize the radiation field to which the particle cloud system was exposed. Neglecting spectral effects, the field may be described by the flux distribution and the total amount of radiant energy impinging on the aerosol conduit. The flux distribution was given in an earlier report, but the absolute intensity of the field was not then reliably determined. In recent experiments, the total amount of radiant energy impinging on the aerosol conduit was evaluated by calorimetric measurements using water flowing through the system with the walls of the conduit blackened to absorb all incident energy. The total energy absorbed divided by the surface area of the conduit gave the average flux; it was found to be 21,500 Btu/hr ft^2. This number now permits a more accurate evaluation of the efficiency of an absorbing cloud.

⌊ The energy absorbed by a cloud passing through the radiant field was determined by two energy-balance procedures.⌋ One was made between the reference conditions and the thermal state of the system at the entrance of the calorimeter, and the other was made between the conditions at the reference point and the calorimeter exit. The former involved a calculation of the enthalpy

1

increase of the aerosol system with only air flowing and then with particles

present. The difference between these results gave the net effect of the

particles and the radiant energy absorbed by them. The second energy balance

involved the same procedure except a calculation for the calorimeter coolant

had to be taken into account also.

$\mathcal{L}$ Results were obtained for aerosols of different size fractions of ferrous

sulfide and cupric oxide.$^{\rfloor}$ The particle sizes of each ranged from 25 microns to

approximately 100 microns. The heat transfer data showed that the absorption

of radiation was essentially a linear function of concentration up to about

50 per cent by weight particles and that the absorption increased with decreas-

ing particle size. The particles were described in terms of minimum, mean, and

maximum dimensions. These characteristic measures were determined with the ex-

pectation that they will be used in future analyses.

More recent efforts have been directed toward evaluating from low temper-

ature nitrogen adsorption techniques the surface properties of the powders.

Specifically, the standard BET method, as well as a modified form of it, were

utilized to determine the contribution of internal surface area to radiation

absorption. It was anticipated that these total surface areas combined with

statistical measurements of particle dimensions would permit more complete

understanding of how absorption occurred. Results as yet are not conclusive,

but it appears that external surface area may be the significant parameter after

all. The problem is still being investigated.

To help resolve questions about particle surface area and the attenuation

of radiation, a mathematical model is being developed from the basic equations

of radiant heat transfer to describe the energy absorbed by a particle cloud

in a circular cylinder. The development is being made in two steps. One is

2

to be valid when radiant energy scattering can be neglected and the second is a modification to estimate these effects as they become more pronounced. Major efforts are being concentrated on this analysis at the moment.

II. INTRODUCTION

The thermal behavior of particle clouds during exposure to a radiant heat field is being studied. The ultimate goal is a quantitative description of the basic processes involved. It is anticipated that the results will be applied to practical problems, especially those in which aerosols within a cylindrical enclosure are exposed to thermal radiation both for purposes of protection and energy utilization. This report presents the experimental data collected during the fourth reporting period of the project and describes the processes currently being examined for analyzing the results. Data reduction methods are also discussed.

Familiarity with apparatus and procedures previously reported is presumed.

III. INVESTIGATIONS

A. Radiant Heat Flux Determinations

Basic to all heat transfer calculations in this study is the radiant heat flux penetrating the quartz enclosures and traversing the particle cloud. To determine this quantity, experiments were conducted in which water was forced to flow upward through the quartz to remove the heat absorbed by the system from the radiant field. To assure total absorption of the impinging radiation, the inner surface of the quartz conduit was coated with a thick slurry of graphite suspended in a solution of plexiglass in ethylene dichloride. Upon evaporation of the solvent, a continuous film of graphite suspended in plexiglass was produced having a thickness of approximately 1 mm.

With the furnace at operating temperature (2160°F), a water flow rate of 0.374 GPM was established through the 0.5 inch diameter quartz conduit. The temperature of the water was determined both at the entrance and the exit of the conduit. The average of several measurements indicated that the water picked up 54.6 Btu/min of energy. This number includes the amount of energy that was absorbed by the quartz wall, which in this case was 5.0 Btu/min. Therefore, the net energy reaching the conduit was 49.6 Btu/min and corresponded to a radiant heat flux at the quartz conduit wall of 21,500 Btu/hr ft^2. This method of determining the total radiant heat flux is considered more reliable than the previous one using a thermocouple probe consisting of an exposed and a shielded thermocouple[1].

The calculations for the previously described technique using a thermo-couple probe involved the use of the emissivity of the exposed bead, which,

---

[1] A. McAlister, H. C. Ward, A. F. Hidalgo and C. Orr, Jr., <u>Heat Transfer to a Gas Containing a Cloud of Particles</u>, Semiannual Status Report No. 3, Project No. A-635, Engineering Experiment Station, Georgia Institute of Technology, Atlanta, Georgia, June 15, 1963, p. 33 ff.

unfortunately, was unknown. The surface of the bead was coated with a thin layer of carbon particles and its emissivity was assumed to be 0.95. With this assumption a distribution of the radiant heat flux along the quartz conduit was calculated for given conditions of free stream air velocity. Graphical integration of this curve yielded an average radiation flux of 7415 Btu/hr ft^2. Although this number is apparently seriously in error, the technique has the value of indicating the profile of the radiation flux. That is, it revealed that there were no sharp discontinuities at the ends and that the distribution of energy was approximately flat for most of the length of the quartz conduit.

B. Energy Balance Procedures

1. Energy Balance at the Entrance of the Calorimeter

The energy absorbed by aerosols was determined by calorimetric measurements. Two energy balances were employed. The first one was made between the reference state and the thermal conditions at the entrance of the calorimeter. Special methods were required to evaluate the temperatures.

The temperature of the aerosol itself was measured by a thermocouple installed 6.5 inches from the entrance of the calorimeter. Previous experiments with this thermocouple were not successful because of radiation reaching into the calorimeter. For these experiments, therefore, the thermocouple was protected from radiation by means of a shield installed at the end of the quartz conduit. The temperature of the aerosol stream at the entrance of the calorimeter was calculated by assuming a linear temperature distribution for the aerosol along the calorimeter. For each test this number was calculated from temperatures measured 6.5 inches downstream from the entrance of the calorimeter and the simultaneously determined temperature at the exit.

The energy balances were set up by taking the reference temperature as that

of the stream at the exit of the aerosol generator and was effectively the same as the temperature of the aerosol at the entrance of the furnace. The base temperature was assumed constant for the purpose of establishing energy balances. Actually, variations in this temperature were present but never exceeded one or two degrees over a period of several hours and not more than a few tenths of a degree over the duration of a test.

With the temperatures described and a knowledge of the individual components of the aerosol, energy balances over the entrance of the calorimeter could be established. The enthalpy change of the air in the stream relative to that of the air with no particles flowing is

$$\Delta H_{1A} = (H_1^1 - H_0^1)_A - (H_1^0 - H_0^0)_A \tag{1}$$

where the subscripts (A,o,1) and superscripts (o,1) indicate the following:

A = a property of the air,

o = the property evaluated at the furnace inlet,

1 = the property evaluated at the calorimeter inlet;

o = evaluation when no particles are flowing,

1 = evaluation when particles are flowing.

With the assumption of a constant base temperature, Equation (1) simplifies to:

$$\Delta H_{1A} = H_{1A}^1 - H_{1A}^0 \tag{2}$$

which in terms of temperatures is

$$\Delta H_{1A}^1 = (w\bar{c})_A (T_{1A}^1 - T_{1A}^0) \tag{3}$$

where $\bar{C}_A$ is the average heat capacity of the air stream between the temperature levels under consideration, and W_A is the mass flow rate of air.

The enthalpy change of the particle stream is given by the relation

$$\Delta H_{1p} = H_{1p}^1 - H_{op}^1 \tag{4}$$

which may be expressed as:

$$\Delta H_{1p} = (w\bar{C})_p \, (T_{1p}^1 - T_{op}^1) \tag{5}$$

where the subscript p indicates a property of the particles, and $\bar{C}_p$ is the average heat capacity of the particle material between the temperature levels under consideration, and W_p is the powder flow rate.

The total enthalpy gain due to the absorption of energy by particles in the radiant field is, finally, the sum

$$\Delta H_{Total} = \Delta H_{1A} + \Delta H_{1p} \tag{6}$$

2. Energy Balance at the Exit of the Calorimeter

A thermocouple was installed at the end of the calorimeter to sense the temperature of the aerosol stream as it left the calorimeter. A difference thermocouple indicated the temperature rise of the cooling air as it passed through the calorimeter. From a knowledge of these temperature readings and the flow rates of the streams involved, a second energy balance was established that included the heat exchange processes in the calorimeter. The total balance is the sum of the heat effects in the air portion of the aerosol, the particle, and the calorimeter coolant.

For the air composing the aerosol, the enthalpy change relative to that of the air when no particles are flowing is given by

$$\Delta H_{3A} = (H_3^1 - H_o^1)_A - (H_3^o - H_o^o)_A \tag{7}$$

where the subscript 3 indicates the property is evaluated at the calorimeter exit.

Since the base temperature is constant, Equation (7) reduces to:

$$\Delta H_{3A} = H_{3A}^1 - H_{3A}^o \tag{8}$$

or,

$$\Delta H_{3A} = (w\bar{c})_A (T_{3A}^1 - T_{3A}^o) \tag{9}$$

The enthalpy change of the particle stream is

$$\Delta H_{3p} = H_{3p}^1 - H_{3p}^o \tag{10}$$

which can be expressed as

$$\Delta H_{3p} = (w\bar{c})_p \cdot (T_{3p}^1 - T_{3p}^o) \tag{11}$$

The enthalpy change of the cooling air stream is

$$\Delta H_c = (w\bar{c})_c \cdot [(\Delta T_c^1) - (\Delta T_c^o)] \tag{12}$$

or,

$$\Delta H_c = (w\bar{c})_c \cdot \Delta(\Delta T_c) \tag{13}$$

where,

$$\Delta(\Delta T_c) = [(\Delta T_c^1) - (\Delta T_c^o)] \tag{14}$$

The notation, $\Delta(\Delta T_c)$, indicates the difference in temperature rise of the calorimeter coolant measured with and without particles in the aerosol stream.

9

The total enthalpy gain due to the flow of particles through the radiation field is the sum,

$$\Delta H_{Total} = \Delta H_{3A} + \Delta H_{3p} + \Delta H_c \qquad (15)$$

C. Particle Materials and Size Measurements

Particle clouds of powdered zinc in one size range and of ferrous sulfide in three size ranges were studied and reported on previously. One additional ferrous sulfide powder of another size range has been employed, and other investigations have included alumina and cupric oxide powders.

Measurements were made of the minimum, maximum, and the mean particle dimensions of each powder. The results are presented in Figures 1 through 5. The distributions given are complete except for the maximum dimension for the 20 to 30 micron screen size ferrous sulfide and the 44 to 53 micron cupric oxide. Statistical treatment of the data has not yet been completed for these. The results are presented here to show the relative sizes of the materials and their length-to-diameter characteristics. The information will be utilized in future analyses when surface properties, mass mean diameters, and other parameters are developed.

The mean distributions were obtained so that the properties of the powders could be treated on the assumption that the particles were spheres with diameters equivalent to the mean. The maximum and the minimum dimensions were determined so that, in other calculations, the particles could be treated as cylinders and the effect of particle irregularity could be taken into account. The final results in each case will be significantly different because of the differences in the surface and mass functions of the two geometric shapes.
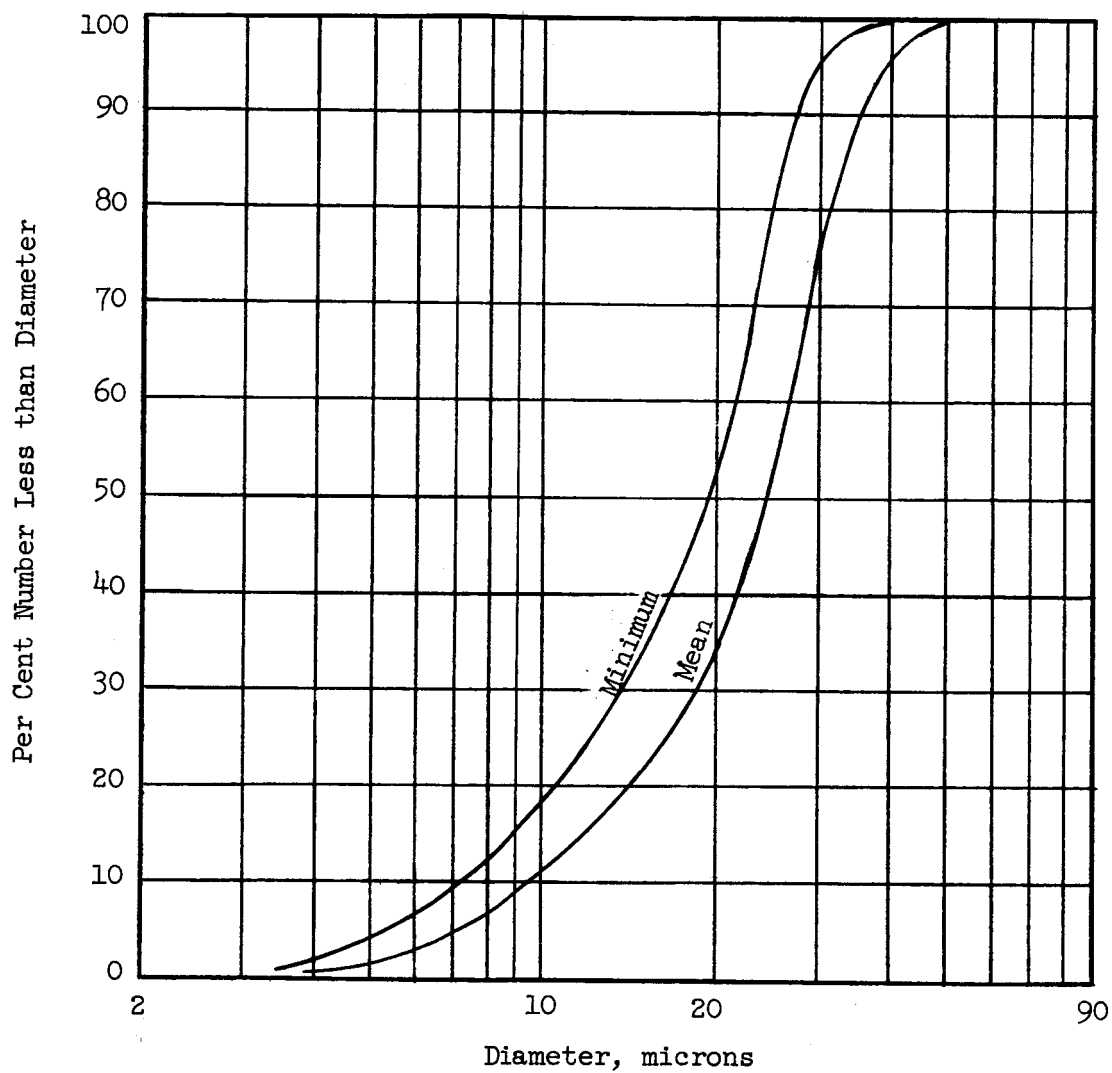
Figure 1. Particle Size Distributions of Ferrous Sulfide,
20-30μ Screen Size Fraction.

11
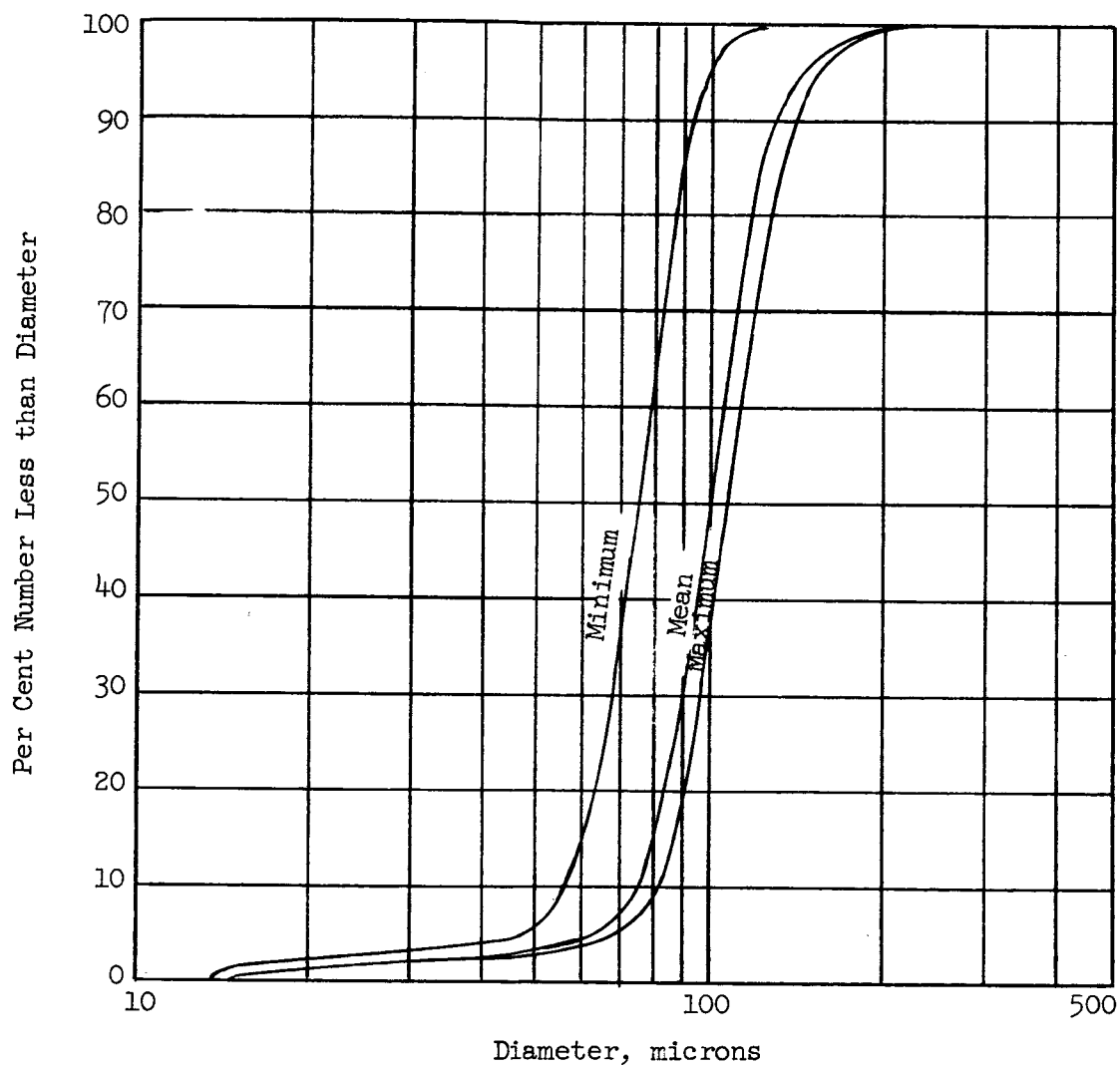
Figure 2. Particle Size Distributions of Cupric Oxide, 53-88μ
Screen Size Fraction.
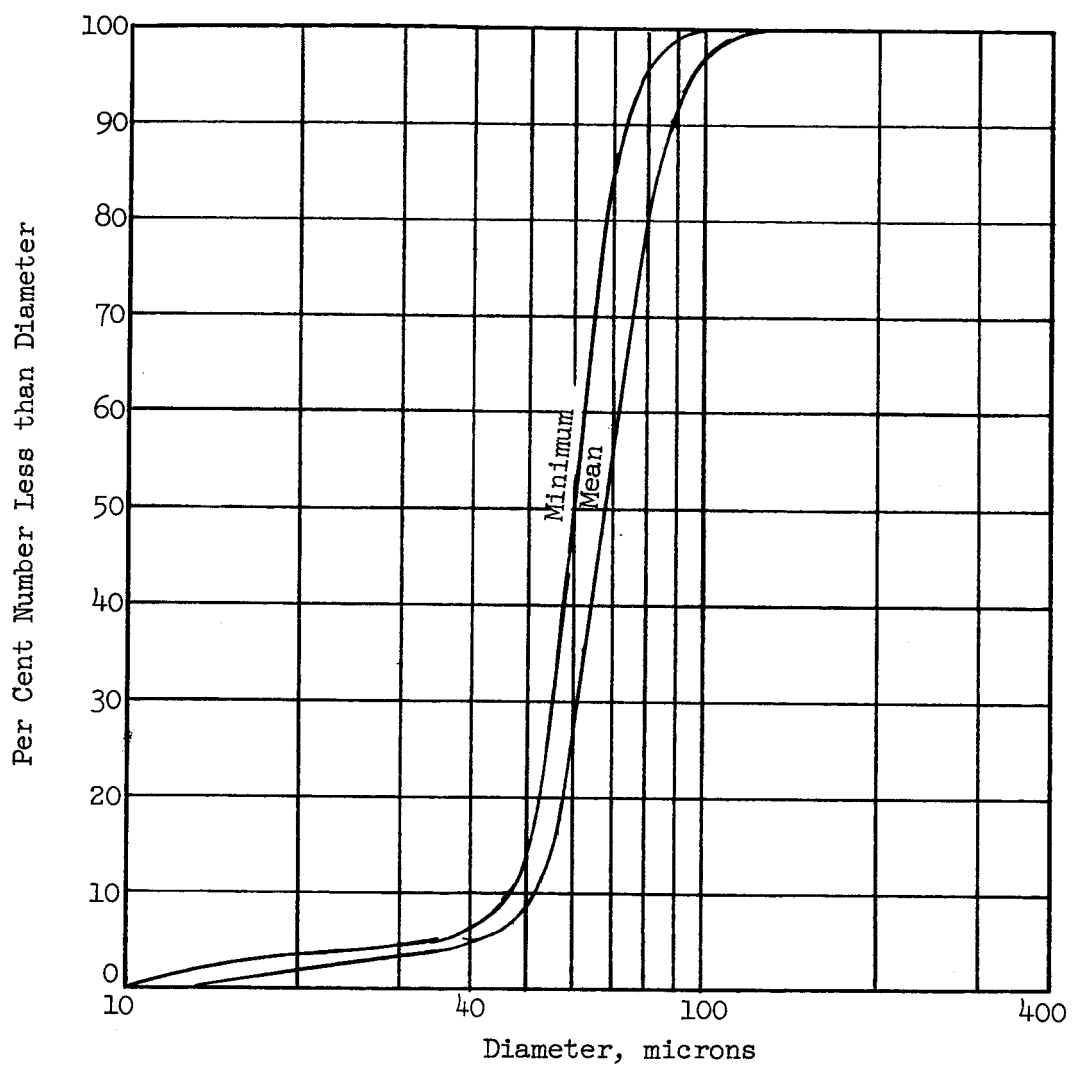
Figure 3. Particle Size Distribution of Cupric Oxide, 44-53µ Screen Size Fraction.
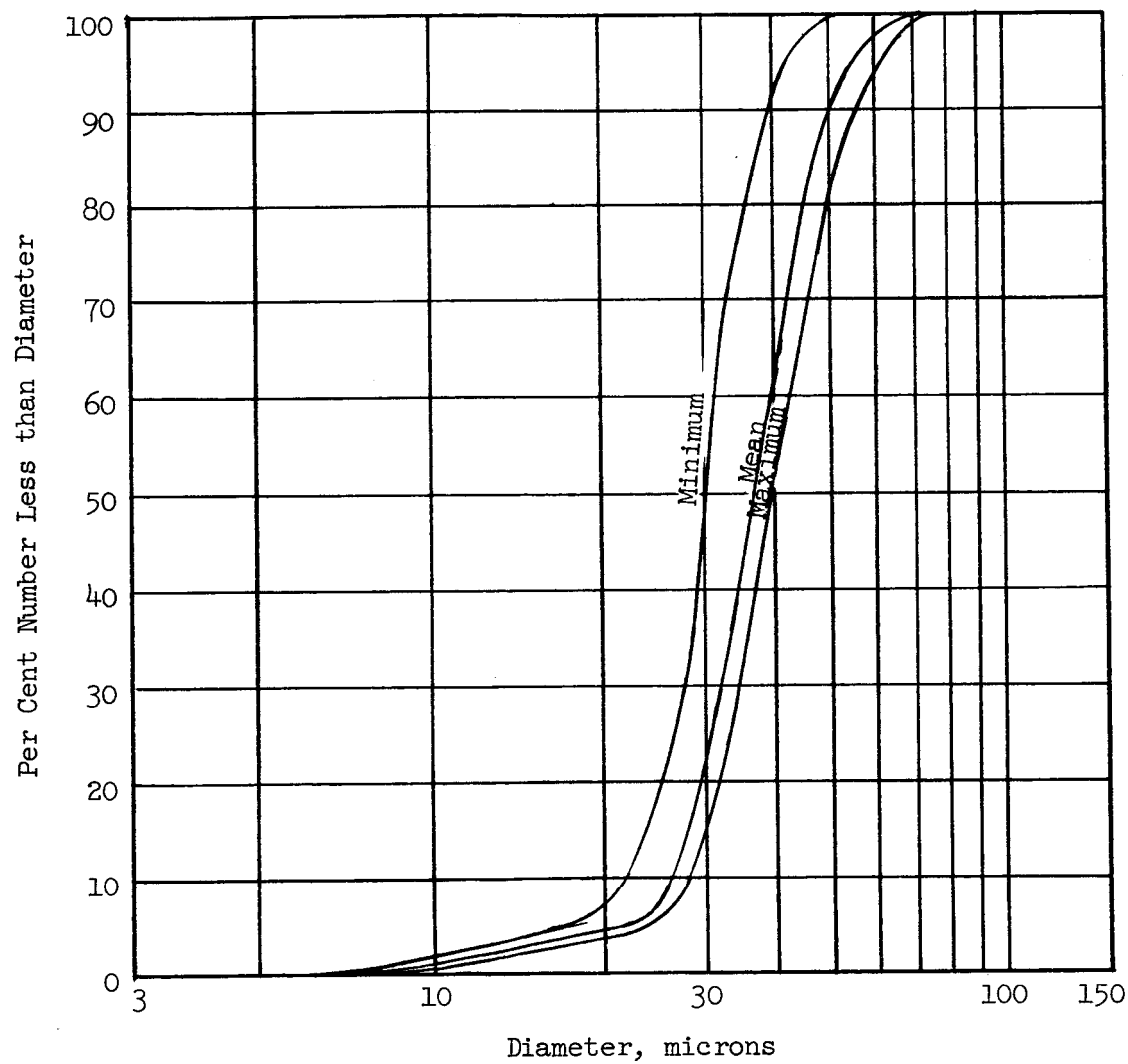
Figure 4. Particle Size Distributions of Cupric Oxide, 30-44μ
Screen Size Fraction.
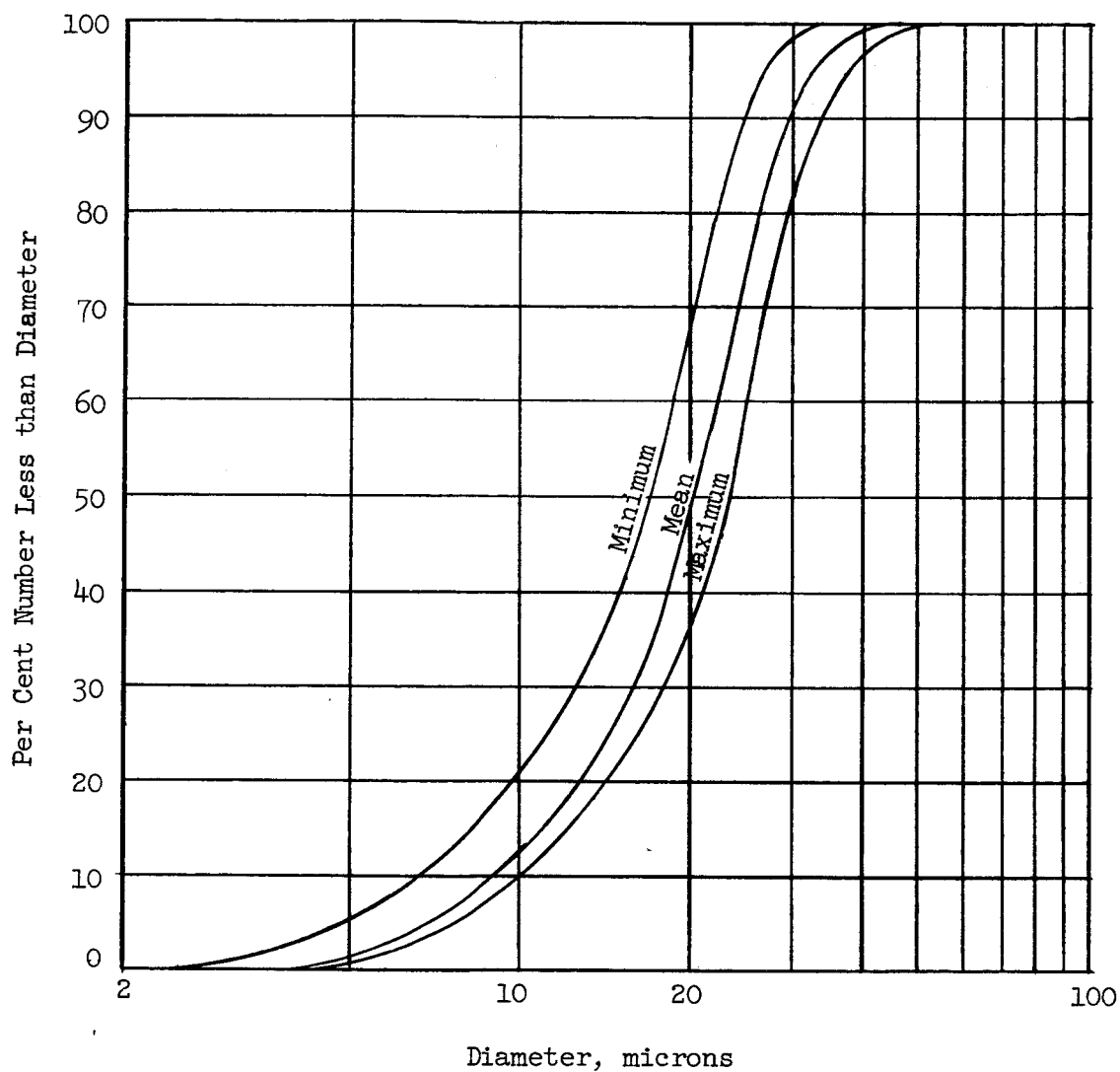
Figure 5. Particle Size Distributions of Cupric Oxide, 20-30µ Screen Size Fraction.

15

D. Heat Transfer Data

Accurate energy balances giving the heat gained by the particle clouds require that the incoming streams not be preheated by contact with the conduit walls. It is equally important that the system not be cooled below the intended base temperature while in the entrance section. These conditions were met by cooling the entrance section so as to keep its wall temperature constant. Tap water was employed as the coolant in previously reported experiments. Except for one experiment, the tap water temperature was sufficiently close to the air temperature to give satisfactory results. For the tests using 30 to 44μ ferrous sulfide, the water was at a sub-normal temperature and the temperature of the aerosol at the entrance of the furnace had to be calculated. The numbers obtained appear reasonably reliable when compared with the temperature of the stream at the entrance of the furnace as determined experimentally[2]. For one test the temperature of the stream at the entrance of the furnace was used as the base temperature for the energy balances. To avoid the recurrence of this complication the apparatus was modified to use air in the precooler. The air from the precooler was also employed to cool the calorimeter. This was possible since the temperature rise of the cooling air on passing through the pre-cooler was negligibly small. After this change the temperature of the aerosol at the entrance of the furnace could always be assumed equal to its temperature measured at the exit of the deagglomerator.

Table I presents data for the 30 to 44μ ferrous sulfide. It is to be noted that these data do not agree with results previously reported. The only explanation is that an air leak in the system caused the concentration of powder in the earlier tests to be higher than reported thus yielding a high radiation

[2] McAlister, A., et al., _Op cit_, p. 48.

TABLE I

DATA FOR 30 TO 44μ FERROUS SULFIDE [a,b]

Test No.	Powder Feed Rate (lb/min)	Stream Temperature At: Deagglomerator Exit Air (°F)	Aerosol (°F)	Furnace Inlet Air (°F)	Aerosol (°F)	Calorimeter Exit Air (°F)	Aerosol (°F)	Calorimeter Coolant Temperature Rise Air, ΔT$_c$ (°F)	Aerosol Δ(ΔT$_c$) (°F)	Enthalpy Change Within System Air (Btu/min)	Particles (Btu/min)	Coolant (Btu/min)	Total (Btu/min)
1	0.156		78.5	53.5	54.7	154.3	171.0	39.7	2.9	0.92	3.08	0.34	4.34
2	0.156		78.8	53.5	54.7	156.2	172.1	40.6	2.8	0.87	3.11	0.33	4.31
3	0.156		78.5	53.5	54.7	155.5	171.0	40.3	2.5	0.85	3.08	0.30	4.23
4	0.089		78.8	53.5	51.7	155.0	168.1	39.8	2.6	0.89	1.77	0.31	2.97
5	0.089		79.0	53.5	51.7	157.1	167.8	40.3	2.1	0.74	1.77	0.25	2.76
6	0.089		79.6	53.5	51.7	158.0	170.1	40.7	2.5	0.83	1.80	0.30	2.93
7	0.242		80.3	53.5	57.3	160.0	186.3	42.0	1.6	1.34	5.32	0.19	6.85
8	0.242		81.1	53.5	57.3	163.0	190.1	43.6	0.4	1.39	5.47	0.05	6.91
9	0.242		80.4	53.5	57.3	159.0	183.8	42.4	1.8	1.25	5.21	0.21	6.67
10	0.242		80.8	53.5	57.3	161.8	191.3	43.4	1.2	1.65	5.52	0.14	7.31
11	0.059		80.5	53.5	50.2	162.2	172.2	43.6	2.0	0.79	1.22	0.24	2.25
12	0.059		81.0	53.5	50.2	162.2	170.1	43.5	1.5	0.68	1.20	0.18	2.06
13	0.059		81.0	53.5	50.2	161.1	170.1	43.4	1.7	0.74	1.20	0.20	2.14

a Experiment Conditions: Calorimeter Cooling Air, 6.36 CFM at 70°F, 1 atm; air flow rate for aerosol, 3.22 CFM at 70°F, 1 atm; precooler water at 49.3°F; furnace temperature 2160°F.

b Energy balance between furnace inlet and calorimeter exit.

17

absorptance.

At this point in the experimental work, a radiation shield was developed which could be installed at the exit of the aerosol stream from the furnace, thereby preventing appreciable radiation from penetrating into the calorimeter. For subsequent experiments, the temperature of the aerosol or air stream was measured by a thermocouple located axially 6.5 in. from the entrance of the calorimeter. Hence, by assuming a linear temperature distribution of the aerosol stream through the calorimeter, it was possible to calculate the aerosol's temperature at the entrance of the calorimeter. An energy balance was then established for the entrance of the calorimeter as well as the exit.

Experiments were then performed with 20 to 30µ micron ferrous sulfide. Some were made with the shield removed and some with the shield in place to detect any adverse effects of the modified system. The data presented in Table II were obtained without the shield in place and the data in Tables III and III-A were obtained with it. Results from the modified system were in good agreement with those of Table II as well as those from previous experiments. Figure 6 summarizes the data obtained for the ferrous sulfide. It represents the radiation absorption as a function of concentration for several particle size distributions.

Two experiments were next made using 53 to 88µ and 44 to 53µ alumina particles. Since this material is partly transparent, very small radiation absorptances were obtained. Because some of the data appear to be outside acceptable limits of uncertainty, they are not presented.

Finally, cupric oxide was selected as a test material. Four size distributions were prepared by methods previously reported. Tables IV through VI present the data obtained on the 53 to 88µ, 44 to 53µ, and 30 to 44µ cupric oxide

TABLE II

EXPERIMENTAL AND CALCULATED DATA FOR 20 TO 30μ FERROUS SULFIDE [a,b]

Test No.	Powder Feed Rate (lb/min)	Stream Temperature At: Deagglomerator Exit Air or Aerosol (°F)	Calorimeter Exit Air (°F)	Calorimeter Exit Aerosol (°F)	Calorimeter Cooling Air Change in Temperature Rise when Powder Added $\Delta(\Delta T_c)$, °F	Enthalpy Change Within Test System Air (Btu/min)	Particles (Btu/min)	Cooling Air (Btu/min)	Total (Btu/min)
1	0.156	72.5	156.0	180.4	3.8	1.45	2.86	0.49	4.80
2	0.156	72.0	156.3	179.1	3.8	1.36	2.84	0.49	4.69
3	0.156	71.7	157.2	179.0	3.8	1.30	2.84	0.49	4.63
4	0.156	71.4	157.7	179.2	3.8	1.28	2.86	0.49	4.63
5	0.156	71.4	155.0	179.0	3.8	1.43	2.85	0.49	4.77
6	0.089	70.6	155.0	171.3	2.6	0.97	1.53	0.34	2.84
7	0.089	71.4	160.0	174.1	2.6	0.84	1.56	0.34	2.74
8	0.089	73.4	162.0	177.2	2.6	0.90	1.58	0.34	2.82
9	0.089	74.9	164.0	179.2	2.6	0.90	1.59	0.34	2.83
10	0.059	75.8	164.5	177.2	1.9	0.76	1.01	0.25	2.02
11	0.059	75.6	162.2	175.0	1.9	0.76	0.99	0.25	2.00
12	0.059	75.2	162.0	174.1	1.9	0.72	0.99	0.25	1.96
13	0.059	75.6	162.8	173.3	1.9	0.63	0.98	0.25	1.85
14	0.242	76.1	165.8	197.1	5.3	1.86	4.99	0.69	7.54
15	0.242	76.3	165.8	196.7	5.3	1.84	4.96	0.69	7.49
16	0.242	76.4	163.7	194.8	5.3	1.85	4.88	0.69	7.42

a. Flow rates: cooling air 7.05 CFM and aerosol air 3.22 CFM at 70°F and 1 atm. Furnace temp: 2160°F.

b. Energy balance between furnace inlet and calorimeter exit.

TABLE III

EXPERIMENTAL AND CALCULATED DATA FOR 20 TO 30μ FERROUS SULFIDE [a,b]

Test No.	Powder Feed Rate (lb/min)	Stream Temperature At: Deagglomerator Exit Air or Aerosol (°F)	Calorimeter Inlet Air (°F)	Calorimeter Inlet Aerosol (°F)	Enthalpy Change Within Test System Air (Btu/min)	Enthalpy Change Within Test System Particles (Btu/min)	Enthalpy Change Within Test System Total (Btu/min)
1	0.156	84.3	218.1	231.0	0.77	3.89	4.66
2	0.089	84.5	221.4	233.2	0.70	2.26	2.96
3	0.089	85.0	223.5	236.4	0.77	2.30	3.07
4	0.089	85.0	223.9	238.8	0.89	2.34	3.23
5	0.156	84.5	227.5	244.0	0.98	4.23	5.21
6	0.156	85.8	221.9	242.3	1.21	4.15	5.36
7	0.156	88.4	225.1	243.2	1.08	4.10	5.18
8	0.089	88.4	226.8	240.6	0.82	2.31	3.13
9	0.059	88.4	225.7	239.0	0.79	1.51	2.30
10	0.059	88.4	226.7	238.0	0.67	1.50	2.17

a Experiment Conditions: calorimeter and precooler cooling air, 6.96 CFM at 70°F, 1 atm; air flow rate for aerosol, 3.22 CFM at 70°F, 1 atm; furnace temperature, 2160°F.

b Energy balance between furnace inlet and calorimeter inlet.

TABLE III-A

EXPERIMENTAL AND CALCULATED DATA FOR 20 TO 30μ FERROUS SULFIDE [a,b]

Test No.	Powder Feed Rate (lb/min)	Stream Temperature At: Deagglomerator Exit Air or Aerosol (°F)	Calorimeter Exit Air (°F)	Aerosol (°F)	Calorimeter Coolant Temperature Rise Air, ΔT_c (°F)	Aerosol, $\Delta (\Delta T_c)$ (°F)	Enthalpy Change Within System Air (Btu/min)	Particles (Btu/min)	Coolant (Btu/min)	Total (Btu/min)
1	0.156	84.3	142.8	174.2	33.6	2.9	1.87	2.38	0.37	4.62
2	0.089	84.5	145.2	166.2	35.1	2.3	1.25	1.24	0.30	2.79
3	0.089	85.0	146.6	169.0	35.2	2.8	1.33	1.28	0.36	2.97
4	0.089	85.0	146.8	169.8	35.2	3.7	1.37	1.29	0.48	3.14
5	0.156	84.5	150.0	185.1	36.7	3.3	2.09	2.67	0.42	5.18
6	0.156	85.8	146.8	184.6	35.7	3.8	2.25	2.62	0.49	5.36
7	0.156	88.4	150.0	186.1	35.3	3.9	2.15	2.59	0.50	5.23
8	0.089	88.4	150.0	172.2	35.4	3.3	1.32	1.27	0.42	3.01
9	0.059	88.4	150.2	166.2	36.1	2.9	0.95	0.78	0.37	2.10
10	0.059	88.4	150.0	165.8	36.1	2.9	0.94	0.77	0.37	2.08

a Experiment Conditions: Calorimeter and precooler cooling air, 6.96 CFM at 70°F and 1 atm; air flow rate for aerosol, 3.22 CFM at 70°F, 1 atm; furnace temperature, 2160°F.

b Energy balance between furnace inlet and calorimeter exit.

Figure 6. Radiant Energy Absorption by Ferrous Sulfide
Particle Clouds. The points are averages of
from 3 to 13 test results.

TABLE IV

EXPERIMENTAL AND CALCULATED DATA FOR 53 TO 88μ CUPRIC OXIDE [a,b]

Test No.	Powder Feed Rate (lb/min)	Stream Temperature At:			Enthalpy Change Within Test System		
		Deagglomerator Exit Air or Aerosol (°F)	Calorimeter Inlet Air (°F)	Aerosol (°F)	Air (Btu/min)	Particles (Btu/min)	Total (Btu/min)
1	0.101	73.0	216.0	207.4	-0.52	1.83	1.31
2	0.101	72.8	216.0	204.9	-0.67	1.80	1.13
3	0.101	73.9	218.7	206.1	-0.76	1.81	1.05
4	0.101	74.0	219.4	206.8	-0.76	1.81	1.05
5	0.101	74.6	221.4	209.7	-0.71	1.83	1.12
6	0.101	74.9	223.2	210.5	-0.77	1.85	1.08
7	0.181	75.8	219.6	199.5	-1.21	3.01	1.80
8	0.181	75.9	220.5	201.8	-1.13	3.06	1.93
9	0.181	76.1	223.1	202.0	-1.27	3.06	1.79
10	0.181	77.3	224.3	202.9	-1.29	3.05	1.76
11	0.313	77.5	226.1	192.7	-2.02	4.84	2.82
12	0.313	78.3	228.5	193.2	-2.13	4.83	2.70
13	0.313	78.5	230.2	193.1	-2.24	4.81	2.57
14	0.313	78.5	231.2	195.7	-2.14	4.92	2.78
15	0.313	79.1	233.4	195.5	-2.29	4.88	2.59

a   Experiment Conditions: Calorimeter and precooler cooling air, 7.20 CFM at 70°F, 1 atm; air flow rate for aerosol, 3.22 CFM at 70°F, 1 atm; furnace temperature, 2160°F.

b   Energy balance between furnace inlet and calorimeter inlet.

TABLE IV-A

EXPERIMENTAL AND CALCULATED DATA FOR 53 TO 88μ CUPRIC OXIDE [a,b]

Test No.	Powder Feed Rate	Deagglomerator Exit	Calorimeter Exit		Calorimeter Coolant Temperature Rise		Enthalpy Change Within System			
		Air or Aerosol	Air	Aerosol	Air, ΔT_c	Aerosol, $\Delta(\Delta T_c)$	Air	Particles	Coolant	Total
	(lb/min)	(°F)	(°F)	(°F)	(°F)	(°F)	(Btu/min)	(Btu/min)	(Btu/min)	(Btu/min)
1	0.101	73.0	136.9	145.0	34.1	+0.1	0.49	0.96	+0.01	1.46
2	0.101	72.8	137.0	144.4	32.8	-0.8	0.45	0.96	-0.10	1.31
3	0.101	73.9	137.9	145.2	34.5	-0.4	0.44	0.96	-0.05	1.30
4	0.101	74.0	139.4	145.9	35.2	-1.5	0.39	0.96	-0.20	1.15
5	0.101	74.6	141.1	147.9	35.8	-1.5	0.41	0.98	-0.20	1.19
6	0.101	74.9	141.3	149.3	35.5	-0.6	0.48	0.99	-0.08	1.39
7	0.181	75.8	140.9	149.0	34.8	-2.6	0.49	1.75	-0.35	1.89
8	0.181	75.9	140.5	150.3	35.0	-2.3	0.59	1.78	-0.31	2.06
9	0.181	76.1	142.1	151.4	36.0	-3.0	0.56	1.81	-0.41	1.96
10	0.181	77.3	142.5	152.0	35.8	-2.6	0.57	1.79	-0.34	2.02
11	0.313	77.5	138.6	152.5	36.0	-4.3	0.84	3.11	-0.58	3.37
12	0.313	78.3	140.6	153.5	36.0	-4.7	0.78	3.12	-0.63	3.27
13	0.313	78.5	140.9	154.4	36.0	-4.4	0.82	3.15	-0.59	3.38
14	0.313	78.5	141.4	156.0	37.1	-4.9	0.88	3.22	-0.66	3.44
15	0.313	79.1	143.4	155.1	37.1	-5.5	0.71	3.14	-0.75	3.10

a Experiment Conditions: Calorimeter and precooler cooling air, 7.20 CFM at 70° and 1 atm; air flow rate for aerosol, 3.22 CFM at 70°F, 1 atm; furnace temperature, 2160°F.

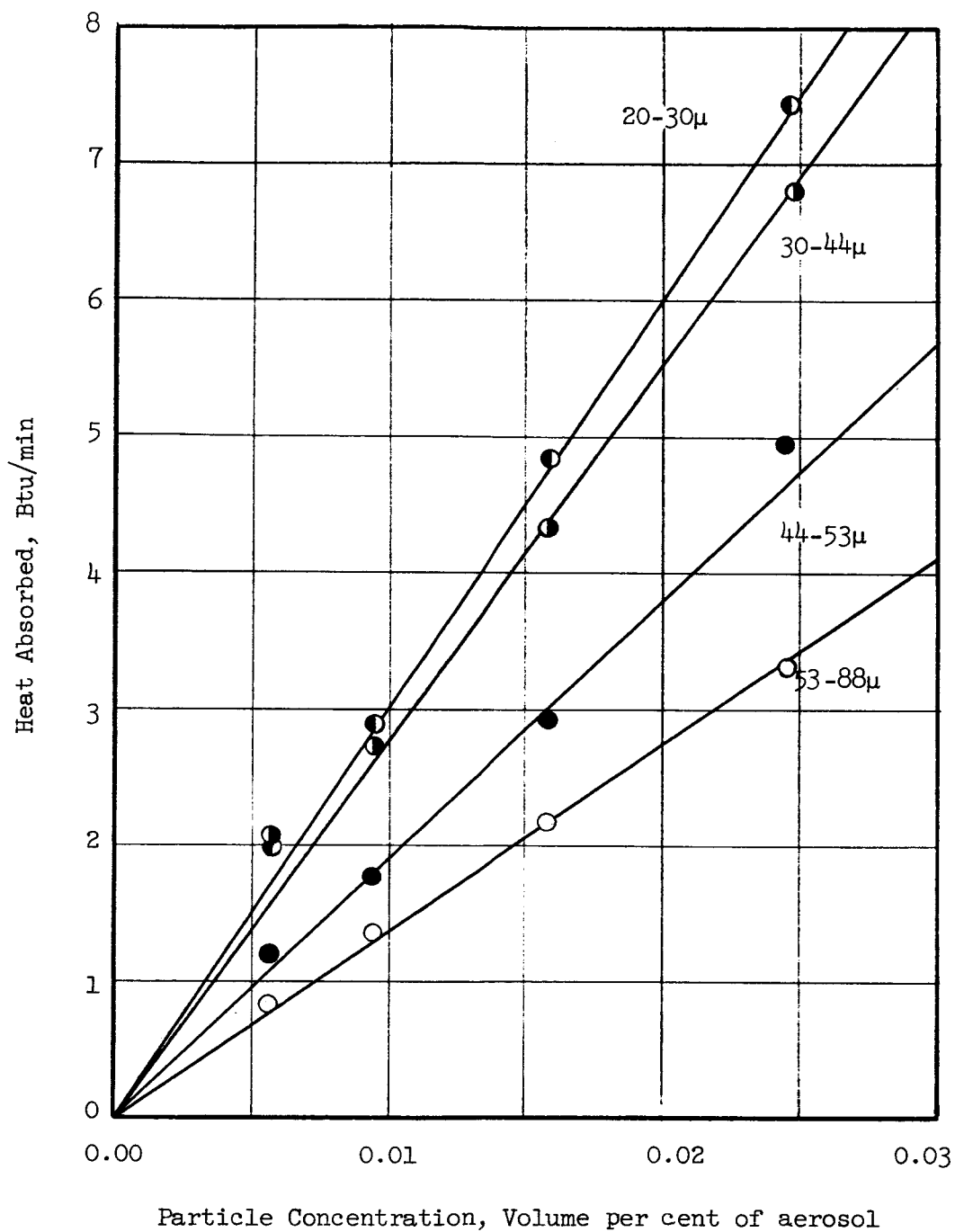b Energy balance between furnace inlet and calorimeter exit.

TABLE V

EXPERIMENTAL AND CALCULATED DATA FOR 44 TO 53μ CUPRIC OXIDE [a,b]

Test No.	Powder Feed Rate (lb/min)	Stream Temperature At:			Enthalpy Change Within Test System		
		Deagglomerator Exit Air or Aerosol (°F)	Calorimeter Inlet Air (°F)	Aerosol (°F)	Air (Btu/min)	Particles (Btu/min)	Total (Btu/min)
1	0.101	70.0	209.4	206.9	-0.14	1.86	1.72
2	0.181	70.9	210.0	200.9	-0.52	3.16	2.64
3	0.181	71.7	207.2	200.6	-0.38	3.13	2.75
4	0.181	72.5	209.4	201.3	-0.46	3.13	2.67
5	0.181	75.0	216.1	207.2	-0.51	3.23	2.72
6	0.181	75.4	216.8	206.6	-0.58	3.20	2.62
7	0.181	75.6	217.1	206.6	-0.60	3.20	2.60
8	0.181	76.2	216.2	206.3	-0.57	3.17	2.60
9	0.181	76.2	217.1	206.3	-0.62	3.17	2.55
10	0.313	77.1	218.7	203.0	-0.90	5.30	4.40
11	0.313	77.2	218.2	202.1	-0.92	5.26	4.54
12	0.313	77.3	219.3	201.8	-1.00	5.24	4.24
13	0.313	77.4	218.5	202.9	-0.89	5.38	4.39

(continued)

25

TABLE V (continued)

EXPERIMENTAL AND CALCULATED DATA FOR 44 TO 53μ CUPRIC OXIDE [a,b]

Test No.	Powder Feed Rate (lb/min)	Stream Temperature At: Deagglomerator Exit Air or Aerosol (°F)	Calorimeter Inlet Air (°F)	Aerosol (°F)	Enthalpy Change Within Test System Air (Btu/min)	Particles (Btu/min)	Total (Btu/min)
14	0.313	77.5	219.2	202.9	-0.93	5.28	4.35
15	0.313	78.0	220.2	204.3	-0.91	5.32	4.41
16	0.181	77.6	221.1	209.0	-0.69	3.21	2.52
17	0.181	77.5	223.0	208.9	-0.81	3.21	2.40
18	0.181	77.0	221.0	208.9	-0.69	3.22	2.55
19	0.101	76.9	219.4	214.5	-0.28	1.87	1.59
20	0.101	76.4	218.3	214.5	-0.22	1.88	1.66
21	0.101	75.8	219.5	213.7	-0.33	1.88	1.55
22	0.101	75.5	220.3	214.5	-0.33	1.89	1.56

a. Experiment Conditions: Calorimeter and precooler cooling air, 7.01 CFM at 70°F and 1 atm; air flow rate for aerosol, 3.05 CFM at 70°F and 1 atm; furnace temperature, 2160°F.

b. Energy balance between furnace inlet and calorimeter inlet.

TABLE V-A

EXPERIMENTAL AND CALCULATED DATA FOR 44 TO 53μ CUPRIC OXIDE [a,b]

Test No.	Powder Feed Rate (lb/min)	Stream Temperature At: Deagglomerator Exit — Air or Aerosol (°F)	Calorimeter Exit — Air (°F)	Calorimeter Exit — Aerosol (°F)	Calorimeter Coolant Temperature Rise, Δ(ΔT)c — Air, ΔTc (°F)	Aerosol (°F)	Enthalpy Change Within System — Air (Btu/min)	Particles (Btu/min)	Coolant (Btu/min)	Total (Btu/min)
1	0.101	70.0	130.0	140.9	34.3	-0.1	0.62	0.93	-0.01	1.54
2	0.181	70.9	131.2	145.4	34.5	-0.8	0.81	1.70	-0.11	2.40
3	0.181	71.7	130.4	145.4	34.1	-0.6	0.86	1.71	-0.08	2.49
4	0.181	72.5	131.4	147.0	33.9	-0.4	0.61	1.73	-0.05	2.29
5	0.181	75.0	136.2	152.1	34.7	-0.6	0.91	1.80	-0.08	2.63
6	0.181	75.4	137.9	151.5	34.9	-0.8	0.78	1.81	-0.11	2.48
7	0.181	75.6	137.0	152.0	34.7	-0.6	0.86	1.81	-0.08	2.59
8	0.181	76.2	137.9	152.7	35.0	-0.9	0.84	1.83	-0.12	2.55
9	0.181	76.2	136.6	152.7	35.1	-1.0	0.92	1.82	-0.13	2.61
10	0.313	77.1	138.3	159.4	35.1	-2.5	1.21	3.20	-0.33	4.08
11	0.313	77.2	137.9	159.4	34.7	-1.5	1.23	3.20	-0.20	4.23
12	0.313	77.3	137.0	159.6	34.8	-1.7	1.29	3.21	-0.22	4.28
13	0.313	77.4	137.0	160.0	35.1	-2.1	1.32	3.21	-0.28	4.25

(continued)

27

TABLE V-A (continued)

EXPERIMENTAL AND CALCULATED DATA FOR 44 TO 53μ CUPRIC OXIDE [a,b]

Test No.	Powder Feed Rate	Stream Temperature At:			Calorimeter Coolant Temperature Rise		Enthalpy Change Within System			
		Deagglomerator Exit Air or Aerosol	Calorimeter Exit Air	Aerosol	Air, ΔT_c	Aerosol, $\Delta(\Delta T_c)$	Air	Particles	Coolant	Total
	(lb/min)	(°F)	(°F)	(°F)	(°F)	(°F)	(Btu/min)	(Btu/min)	(Btu/min)	(Btu/min)
14	0.313	77.5	137.5	160.0	35.1	-1.9	1.29	3.22	-0.25	4.26
15	0.313	78.0	137.9	161.4	35.2	-1.9	1.34	3.25	-0.25	4.34
16	0.181	77.6	138.6	155.1	35.7	-0.6	0.94	1.86	-0.08	2.72
17	0.181	77.5	138.5	155.1	35.5	-0.7	0.95	1.86	-0.09	2.72
18	0.181	77.0	139.5	154.9	35.7	-1.0	0.88	1.85	-0.13	2.60
19	0.101	76.9	137.5	150.0	35.1	+0.1	0.72	1.03	+0.01	1.76
20	0.101	76.4	137.0	150.3	35.4	-0.2	0.76	1.02	-0.03	1.75
21	0.101	75.8	136.2	149.7	34.9	+0.1	0.77	1.01	+0.01	1.79
22	0.101	75.5	137.5	150.0	35.3	0.0	0.72	1.01	0.00	1.73

a Experiment Conditions: Calorimeter and precooler cooling air, 7.01 CFM at 70°F and 1 atm; air flow rate for aerosol, 3.05 CFM at 70°F and 1 atm; furnace temperature 2160°F.

b Energy balance between furnace inlet and calorimeter exit.

TABLE VI

EXPERIMENTAL AND CALCULATED DATA FOR 30 TO 44μ CUPRIC OXIDE [a,b]

Test No.	Powder Feed Rate (lb/min)	Stream Temperature At: Deagglomerator Exit Air or Aerosol (°F)	Calorimeter Inlet Air (°F)	Calorimeter Inlet Aerosol (°F)	Enthalpy Change Within Test System Air (Btu/min)	Enthalpy Change Within Test System Particles (Btu/min)	Enthalpy Change Within Test System Total (Btu/min)
1	0.181	80.8	226.1	212.3	-0.76	3.61	2.85
2	0.181	80.9	226.1	211.4	-0.81	3.59	2.78
3	0.181	81.0	226.2	210.6	-0.86	3.56	2.70
4	0.181	81.0	225.3	211.3	-0.77	3.58	2.81
5	0.181	81.1	226.1	211.3	-0.81	3.58	2.77
6	0.181	81.7	227.3	212.2	-0.83	3.59	2.76
7	0.181	81.8	227.2	213.0	-0.78	3.61	2.83
8	0.181	81.9	228.0	213.0	-0.83	3.60	2.77
9	0.181	81.7	228.0	213.5	-0.81	3.62	2.81
10	0.181	81.9	228.4	214.3	-0.78	3.64	2.86
11	0.181	81.9	228.9	213.0	-0.88	3.60	2.72
12	0.181	81.9	229.0	213.8	-0.84	3.63	2.79
13	0.103	81.9	227.1	221.8	-0.29	2.19	1.90
14	0.103	81.9	226.5	220.6	-0.33	2.17	1.84

(continued)

TABLE VI (continued)

EXPERIMENTAL AND CALCULATED DATA FOR 30 TO 44μ CUPRIC OXIDE [a] [b]

Test No.	Powder Feed Rate (lb/min)	Deagglomerator Exit Air or Aerosol (°F)	Calorimeter Inlet Air (°F)	Aerosol (°F)	Enthalpy Change Within Test System Air (Btu/min)	Particles (Btu/min)	Total (Btu/min)
15	0.103	81.9	227.1	220.4	-0.37	2.17	1.80
16	0.103	82.8	227.1	221.6	-0.30	2.17	1.87
17	0.103	82.8	227.7	221.6	-0.34	2.17	1.83
18	0.103	82.9	226.8	222.0	-0.27	2.18	1.91
19	0.103	83.0	227.7	222.0	-0.31	2.18	1.87
20	0.103	83.4	227.9	222.4	-0.31	2.18	1.87
21	0.103	83.6	251.7	223.2		2.19	
22	0.103	83.6	227.7	223.6	-0.23	2.19	1.96
23	0.103	83.7	227.9	222.9	-0.28	2.18	1.90
24	0.103	83.6	227.9	222.0	-0.33	2.17	1.84
25	0.070	83.6	227.9	225.9	-0.11	1.51	1.40
26	0.070	83.9	227.8	226.4	-0.08	1.52	1.44
27	0.070	84.2	227.8	226.4	-0.08	1.51	1.43
28	0.070	84.5	228.7	227.3	-0.08	1.52	1.44
29	0.070	84.2	229.9	228.0	-0.11	1.53	1.42

(continued)

30

TABLE VI (continued)

EXPERIMENTAL AND CALCULATED DATA FOR 30 TO 44μ CUPRIC OXIDE [a,b]

Test No.	Powder Feed Rate (lb/min)	Stream Temperature At: Deagglomerator Exit Air or Aerosol (°F)	Calorimeter Inlet Air (°F)	Calorimeter Inlet Aerosol (°F)	Enthalpy Change Within Test System: Air (Btu/min)	Particles (Btu/min)	Total (Btu/min)
30	0.070	84.2	230.3	228.5	-0.10	1.54	1.44
31	0.320	84.5	230.0	219.2	-0.60	6.56	5.96
32	0.320	84.9	228.7	219.2	-0.52	6.53	6.01
33	0.320	85.0	229.2	219.2	-0.55	6.53	5.98
34	0.320	84.7	230.0	218.3	-0.65	6.50	5.85
35	0.320	85.0	232.3	221.1	-0.62	6.62	6.00
36	0.320	85.4	232.9	222.4	-0.58	6.66	6.08
37	0.320	85.0	232.7	221.5	-0.62	6.64	6.02
38	0.320	85.0	232.7	222.3	-0.57	6.68	6.11
39	0.320	85.1	232.1	222.0	-0.56	6.67	6.11
40	0.320	85.8	234.5	222.3	-0.68	6.64	5.96
41	0.320	85.2	235.4	224.7	-0.59	6.78	6.19

a Experiment Conditions: Calorimeter and precooler cooling air, 3.04 CFM at 70° F and 1 atm; air flow rate for aerosol, 6.82 CFM at 70°F and 1 atm; furnace temperature, 2160°F.

b Energy balance between furnace inlet and calorimeter inlet.

31

TABLE VI-A

EXPERIMENTAL AND CALCULATED DATA FOR 30 TO 44μ CUPRIC OXIDE [a,b]

Test No.	Powder Feed Rate (lb/min)	Stream Temperature At: Deagglomerator Exit Air or Aerosol (°F)	Stream Temperature At: Calorimeter Exit Air (°F)	Aerosol (°F)	Calorimeter Coolant Temperature Rise Air, ΔT_c (°F)	Aerosol, $\Delta(\Delta T_c)$ (°F)	Enthalpy Change Within System Air (Btu/min)	Particles (Btu/min)	Coolant (Btu/min)	Total (Btu/min)
1	0.181	80.8	143.8	160.1	36.4	-1.3	0.89	2.17	-0.15	2.91
2	0.181	80.9	143.8	160.1	37.0	-2.3	0.89	2.17	-0.28	2.78
3	0.181	81.0	143.0	159.3	36.4	-1.6	0.89	2.14	-0.19	2.84
4	0.181	81.0	143.0	160.5	36.5	-1.6	0.96	2.17	-0.19	2.94
5	0.181	81.1	143.8	160.5	36.6	-1.7	0.91	2.17	-0.21	2.87
6	0.181	81.7	144.6	160.5	36.7	-1.6	0.87	2.16	-0.19	2.84
7	0.181	81.8	145.0	160.9	36.5	-1.3	0.87	2.17	-0.15	2.89
8	0.181	81.9	145.4	161.3	36.9	-1.7	0.87	2.17	-0.22	2.82
9	0.181	81.7	145.4	161.3	36.9	-1.6	0.87	2.18	-0.19	2.86
10	0.181	81.9	146.2	161.7	37.1	-1.7	0.84	2.18	-0.21	2.81
11	0.181	81.9	145.4	161.7	37.1	-1.8	0.89	2.18	-0.21	2.86
12	0.181	81.9	145.0	161.7	37.0	-1.5	0.91	2.18	-0.18	2.91
13	0.103	81.9	145.8	156.8	37.2	-0.5	0.60	1.17	-0.07	1.70
14	0.103	81.9	143.8	156.0	37.0	-0.5	0.67	1.15	-0.06	1.76

(continued)

TABLE VI-A (continued)

EXPERIMENTAL AND CALCULATED DATA FOR 30 TO 44μ CUPRIC OXIDE [a,b]

Test No.	Powder Feed Rate (lb/min)	Stream Temperature At: Deagglomerator Exit Air or Aerosol (°F)	Calorimeter Exit Air (°F)	Calorimeter Exit Aerosol (°F)	Calorimeter Coolant Temperature Rise Air, ΔT_c (°F)	Aerosol, $\Delta(\Delta T_c)$ (°F)	Enthalpy Change Within System Air (Btu/min)	Particles (Btu/min)	Coolant (Btu/min)	Total (Btu/min)
15	0.103	81.9	145.4	156.8	36.9	-0.4	0.62	1.17	-0.05	1.74
16	0.103	82.8	146.2	157.6	36.6	-0.4	0.62	1.17	-0.05	1.74
17	0.103	82.8	147.5	157.6	37.3	-1.1	0.56	1.17	-0.14	1.59
18	0.103	82.9	147.5	158.0	36.8	-0.3	0.58	1.17	-0.04	1.71
19	0.103	83.0	147.5	158.0	37.1	-0.6	0.58	1.17	-0.07	1.68
20	0.103	83.4	145.8	158.4	36.8	-0.3	0.69	1.17	-0.04	1.82
21	0.103	83.6	147.1	159.3	37.1	-0.6	0.67	1.18	-0.08	1.77
22	0.103	83.6	147.5	159.3	36.8	0.0	0.64	1.18	-0.01	1.81
23	0.103	83.7	146.2	158.4	36.9	-0.5	0.67	1.17	-0.06	1.78
24	0.103	83.6	146.2	158.4	36.9	-0.4	0.67	1.17	-0.05	1.79
25	0.070	83.6	146.2	156.4	37.1	-0.1	0.56	0.77	-0.01	1.32
26	0.070	83.9	146.6	156.0	36.8	0.0	0.51	0.76	-0.01	1.26
27	0.070	84.2	146.6	156.0	36.8	-0.1	0.51	0.76	-0.01	1.26
28	0.070	84.5	147.1	156.0	37.3	-0.1	0.49	0.76	-0.01	1.24
29	0.070	84.2	147.9	157.2	37.2	0.0	0.51	0.77	0.00	1.28

(continued)

33

TABLE VI-A (continued)

EXPERIMENTAL AND CALCULATED DATA FOR 30 TO 44μ CUPRIC OXIDE [a,b]

Test No.	Powder Feed Rate (lb/min)	Stream Temperature At: Deagglomerator Exit Air or Aerosol (°F)	Calorimeter Exit Air (°F)	Calorimeter Exit Aerosol (°F)	Calorimeter Coolant Temperature Rise, ΔT_c Air, ΔT_c (°F)	Calorimeter Coolant Temperature Rise Aerosol, $(\Delta T_c)_c$ (°F)	Enthalpy Change Within System Air (Btu/min)	Enthalpy Change Within System Particles (Btu/min)	Enthalpy Change Within System Coolant (Btu/min)	Enthalpy Change Within System Total (Btu/min)
30	0.070	84.2	148.3	156.8	37.3	-0.1	0.47	0.77	-0.01	1.23
31	0.320	8.45	147.5	179.3	37.0	-2.1	1.74	4.60	-0.26	6.08
32	0.320	84.9	147.1	178.9	36.4	-1.5	1.74	4.55	-0.17	6.12
33	0.320	85.0	147.1	179.3	36.7	-2.1	1.76	4.57	-0.26	6.07
34	0.320	84.7	147.1	178.9	36.4	-1.9	1.74	4.56	-0.23	6.07
35	0.320	85.0	149.5	181.3	36.6	-1.3	1.74	4.67	-0.16	6.25
36	0.320	85.4	148.7	181.7	37.9	-2.5	1.80	4.67	-0.30	6.17
37	0.320	85.0	149.5	181.3	37.2	-1.9	1.74	4.67	-0.24	6.17
38	0.320	85.0	149.9	182.1	37.6	-2.3	1.76	4.71	-0.28	6.19
39	0.320	85.1	147.9	186.4	37.4	-2.1	2.11	4.92	-0.25	6.78
40	0.320	85.8	149.5	182.1	37.6	-2.5	1.78	4.67	-0.31	6.14
41	0.320	85.2	149.9	183.6	37.9	-2.2	1.84	4.77	-0.26	6.35

a   Experiment Conditions: Calorimeter and precooler cooling air, 3.04 CFM at 70° F and 1 atm; air flow rate for aerosol, 6.82 CFM at 70° F and 1 atm; furnace temperature 2160°F.

b   Energy balance between furnace inlet and calorimeter exit.

aerosols, respectively, while Figure 7 presents the results graphically. An
additional experiment was carried out using 20 to 30μ cupric oxide, but the data
obtained do not correlate well with previous tests using cupric oxide. The con-
centration of this powder may not have been measured correctly.

E. Thermal Absorption Efficiency

1. Estimates Assuming Isotropic Radiation

If the radiant flux within an aerosol can be determined and if the
particle surface area and the appropriate view factors are known, the thermal
absorption efficiency of the particle cloud may be calculated exactly. For
initial estimates, however, it was assumed that the radiation was isotropic, and
the particle-to-wall view factors were considered unity. These assumptions
were justified for estimations only, and were made to aid initial interpreta-
tions of the experimental data. Particle surface areas were determined by
three methods: microscopic measurements, standard BET nitrogen adsorption, and
a modified procedure to be explained later.

The surface area data are presented in Table VII, and the calculated
absorptivities based on these values and the assumptions involved are given in
Table VIII. As shown, the absorptance efficiency is inversely proportional to
the surface area measurement; it ranges from very small values to greater than
unity. It was hoped that the estimated values might indicate the proper method
for determining surface area. Instead, the problem was complicated since plau-
sible arguments could be given to support any particular method. Absorptivities
based on S_m, the microscopic measurements, were large and variable. Such
variations in absorptivity, however, would not be expected since quantum effects,
which produce the changes, should not arise for such large particles.   The

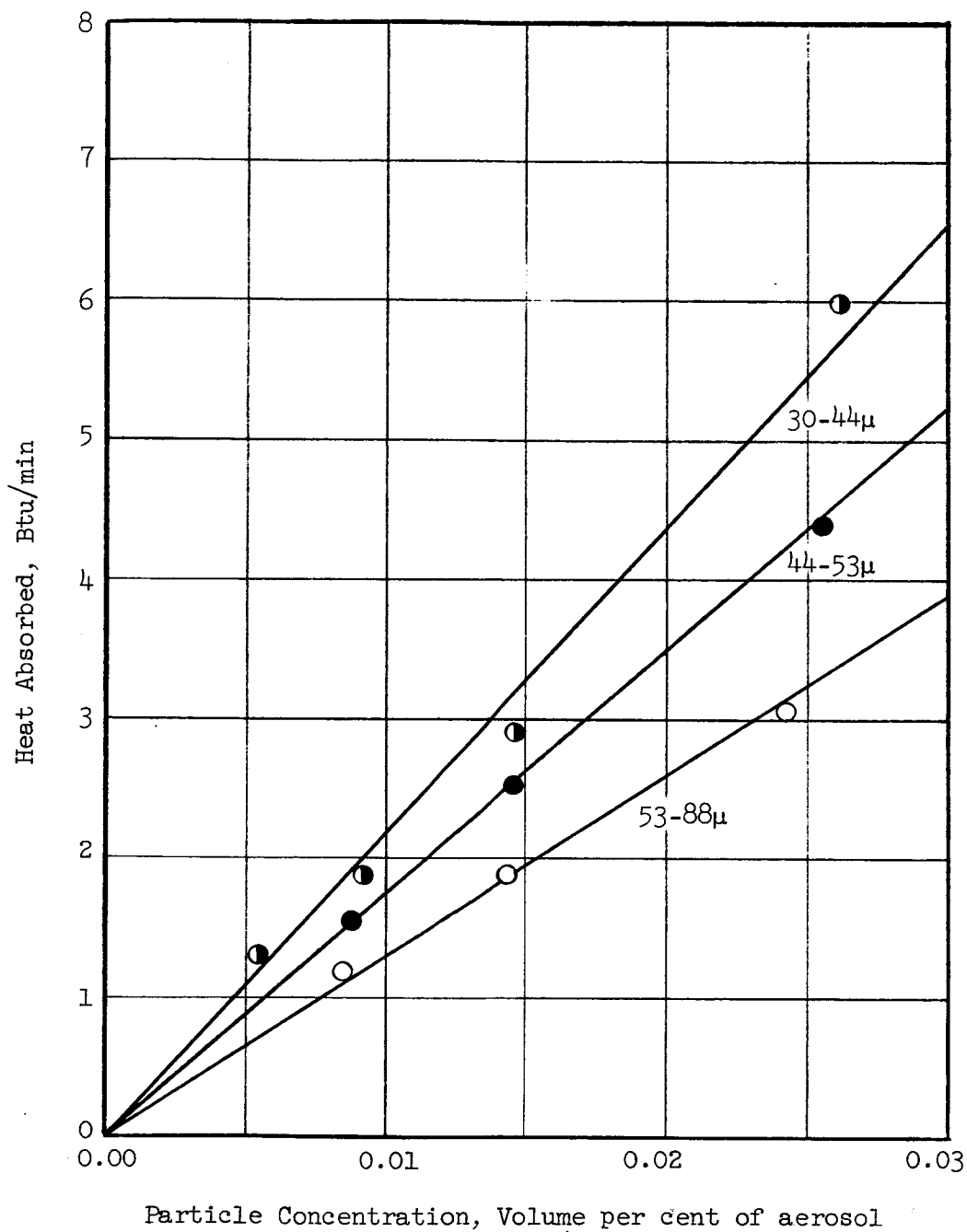Figure 7.   Radiant Energy Absorption by Cupric Oxide
             Particle Clouds. The points are averages
             of from 8 to 24 test results.

TABLE VII

SURFACE AREAS FOR POWDERED
MATERIALS DETERMINED BY DIFFERENT METHODS

Material	Screen Size Designation (μ)	Surface Areas, m^2/gm		
		S_w[a] (m^2/gm)	(S_w-S_p)[b] (m^2/gm)	S_m[c] (m^2/gm)
FeS	53-88	0.13	0.04	0.016
FeS	44-53	0.14	0.05	0.02
FeS	30-44	0.23	0.08	0.03
FeS	20-30	0.24	0.08	0.05
CuO	53-88	0.10	-0.07	0.015
CuO	64-53	0.20	0.00	0.02
CuO	30-44	0.21	0.02	0.04

[a] BET nitrogen adsorption surface area

[b] Adjusted BET results (see text)

[c] Surface area from particle measurement.

TABLE VIII

THERMAL ABSORPTION EFFICIENCY BASED
ON DIFFERENT METHODS OF SURFACE MEASUREMENT

Material	Screen Size Designation	Thermal Absorption Efficiency Based On Surface Areas Indicated by		
		S_w	(S_w-S_p)	S_m
FeS	53-88	0.14	0.5	1.18
FeS	44-53	0.18	0.5	0.86
FeS	30-44	0.17	0.5	0.60
FeS	20-30	0.11	0.3	0.49
CuO	53-88	-.08	-	0.53
CuO	44-53	0.05	0.0	0.54
CuO	30-44	0.06	0.7	0.33

BET adsorption surface areas, Sw, on the other hand, yielded absorptivities much too small. If it is considered that polished metal surfaces have absorptivities around 0.05 to 0.07 and, with dull finishes, have values as high as 0.4, then, ferrous sulfide and cupric oxide, both being non-conductors, should, according to electromagnetic theory, have larger absorptivities. Eckert[3] gives 0.8 as the absorptivity for low temperature radiation for cupric oxide.

Although factors other than the particle surface area can significantly influence the results, it was suspected that the proper value had not been obtained, and that the correct one lay between Sw and Sm. Normally, results from microscopic measurements are smaller than obtained by other methods. This is because the particles are assumed to have a regular geometry and the surface calculated does not consider the irregularities in particle shape. BET results can be too large since the total surface is measured and some of this surface is internal, as in pores, surface cracks, and crystallographic imperfections. The area associated with these internal irregularities can be studied by an extended BET analysis generally referred to as a pore volume determination. A number of experiments were performed to determine if the technique would be useful in this study.

In a gas adsorption surface area measurement, a determination is made of the number of molecules of a gas, usually nitrogen, required to cover a surface with a monolayer of molecules. The total surface is evaluated assuming the area covered by a single nitrogen molecule is known. By extending the adsorption procedure beyond the mono-molecular coverage, attaining saturation, and then desorbing to the monolayer state again, the portion of the surface that is

---

[3] E. R. G. Eckert and R. M. Drake, Jr., *Heat and Mass Transfer*, McGraw-Hill Book Co., Inc., New York, 1959, p.377.

internal can be estimated. The details of the procedure are reviewed elsewhere[4][5].

Column four of Table VIII gives surface areas adjusted for porosity, i.e., (Sw - Sp) values which represent the surface surrounding the particles. The results appear in the order they were obtained. As shown, the earlier results appear to yield good values for radiation absorptance efficiencies. However, later measurements, principally those for cupric oxide, are not encouraging, since Sp is as large as Sw and in some cases larger. These unrealistic results may be due to the presence of moisture in the adsorbate used. This moisture would condense in the sample holder at liquid nitrogen temperature and hence would not come off upon desorption. This explains the unreasonably high pore surfaces obtained. The problem is still being investigated and consideration is being given to a repeating of the experiments after steps have been taken to avoid contamination of the adsorbate. Should the final BET results prove unrealistic, it will be necessary to use statistical results from the microscopic examinations.

2. Anisotropic Radiation

Since there are other factors which can affect the absorption efficiency of a particle cloud, the results of Table IX must be evaluated further. Observations of experiments while in progress indicated that the particle clouds had very large optical thicknesses. Hence it appeared that attenuation of radiant energy, as a first approximation, might be neglected. As the next

[4] C. Orr, Jr., and J. M. DallaValle, Fine Particle Measurement, Size, Surface, and Pore Volume, The Macmillan Co., New York, 1959, p. 257 f.

[5] P. H. Emmett [editor], Catalysis, Vol. II, Fundamental Principles (Part 2), New York, 1955, p. 105 f.

step, a development is being pursued which considers radiant energy attenuation but still omits scattering effects. The approach being employed is to integrate the basic relationship describing the exchange of radiant energy between two elemental areas separated by a given distance which is a function of the position of a particle within the radiation field and the point at which radiation enters the particle cloud. The development is partially complete. The mechanics of the integration process have been worked out but a final solution has not been obtained.

Numerical results accounting for attenuation should be exact if there is no scattering of radiant energy. It is anticipated that ammendments can be made to approximate the effects of scattered radiation by changing the attenuation function. Specifically, if radiation can be considered to be represented by

$$I_2 = I_{1x} e^{-kx} \tag{16}$$

where I_2 and I_1 are the intensities of radiation at positions two and one along the straight line x and k is the attenuation constant, then

$$I_2 = I_{1x} e^{-k_1 x} \tag{17}$$

where scattering is significant. k_1 is larger than k because each particle, by virtue of scattering, adds to the energy proceeding in the x direction. If a scattering function is assumed for a given particle, k_1 can be evaluated in terms of k, however.

IV. FUTURE WORK

Future efforts will be concentrated on developing methods for calculating the amount of radiant energy that a particle cloud should absorb in the experimental system. These calculations will be made first to account for radiant energy attenuation within the cloud and second to estimate the effects of radiation scattering by individual particles. It will then be possible to re-examine the various methods of surface area determination and evaluate the one best suited for this problem.

The collection of additional experimental data will be resumed when the theoretical developments permit evaluating the significance of the data already collected.

Respectfully submitted:

Clyde Orr

Clyde Orr
Project Director

Approved:

Frederick Bellinger

Frederick Bellinger, Chief
Chemical Sciences and Materials Division